[Article ID] 1003- 6326(2001) 01- 0040- 05

Effect of coupling between melt shape and temperature field on electromagnetic shaping[©]

SHEN Jun(沈 军)¹, PEI Xim feng(裴新风)², HOU Jiam ping(侯建平)¹, LI Jiam guo(李建国)¹, FU Heng zhi(傅恒志)¹

- (1. State Key Laboratory of Solidification Processing, Northwestern Polytechnic University, Xi an 710072, P. R. China;
- Department of Computer Science and Engineering, Northwestern Polytechnic University, Xi an 710072, P. R. China)

[Abstract] Based on the analyses of electromagnetic pressure on melt and heat induced in melt, the ratio of heat to pressure $Q_0/p_{\rm m}$ was defined. It was given that the relationship between $Q_0/p_{\rm m}$ and thickness a, electromagnetic parameter $\mu_{\rm Y}$ of melt and electric current frequency f under electromagnetic confinement and shaping process. If the value of $Q_0/p_{\rm m}$ is big, any adjustment on melt shape will easily cause a variation of temperature in melt. In this situation, there appears a more sensitive interaction between shape and temperature field and a more narrow adjustment range for this process. Experiments on some thin plate samples with a cross-section of $6\,{\rm mm}\times 18\,{\rm mm}$ have been done in two kinds of induction coils respectively. The results show that as the coil with a trumpet inside wall is used and the positions of melt top and S/L interface are properly selected, the melt periphery is nearly vertical and the temperature gradient ahead of S/L interface is high. On this condition, a more stable and wider coupling between shape and temperature field has been continuously maintained and samples with smooth surface and unidirectional crystals have been successfully obtained.

[Key words] electromagnetic shaping; temperature field; melt shape; coupling

[CLC number] TG 132. 3

[Document code] A

1 INTRODUCTION

The electromagnetic casting technique was applied to obtaining aluminum ingots with large crosssection in 1980, in which low electric current frequency was usually selected^[1~5]. In our laboratory, the research is focused on the electromagnetic shaping of blade-like and thin plate casting recently. It is known that in order to hold a given shape of melt the magnetic field should be adjusted instantly at all time. For ingot with large cross-section, the variation of magnetic flux density just has a little effect on temperature field^[6~8]. But for those with thin crosssection, the variation of magnetic flux density will cause an obvious change of temperature in melt, which leads the move of position of S/L interface. The displacement of S/L interface changes the relationship between the static pressure of melt and the electromagnetic pressure and makes the melt shape vary unexpectedly. Similar unexpected variation of melt shape also happens while the temperature is adjusted by changing the magnetic field. This is because of a significant effect of magnetic field on both electromagnetic pressure and temperature. Therefore, it is not considered to be possible to adjust the melt shape or temperature field without influencing each other. By comparison, the process of electromagnetic confinement and shaping for thin plate has two new characteristics: 1) the magnetic flux density plays the same important roles in heating and shaping; 2) the melting and shaping can be completed simultaneously by a single induction coil. In this study, the ratio of heat to pressure is defined and discussed. The interaction between shape and temperature field of melt is also investigated with experiments.

2 THEORETICAL ANALYSES

In former research works^[9,10], we have brought forward the equations about induced current density in melt and electromagnetic pressure on melt in electromagnetic confinement and shaping of plate. Equation (1) and equation (2) in the following are for induced current density J_y in plate melt and for electromagnetic pressure p_m on plate melt respectively:

$$J_{y} = B \sqrt{\frac{2\pi f \, Y(\cosh 2Kx - \cos 2Kx)}{\mu(\cosh Ka + \cos Ka)}}$$
(1)
$$p_{m} = \frac{B^{2}}{2\,\mu} \frac{1}{\cosh Ka + \cos Ka} \int_{0}^{Ka} \sqrt{\cosh^{2}t - \cos^{2}t} \, dt$$
(2)

where $K = \sqrt{\pi f \mu_Y}$. As shown in Fig. 1, B is the magnetic flux density on the periphery of melt, a is the thickness of melt, f is the current frequency, and μ and γ are the magnetic conductivity and electric

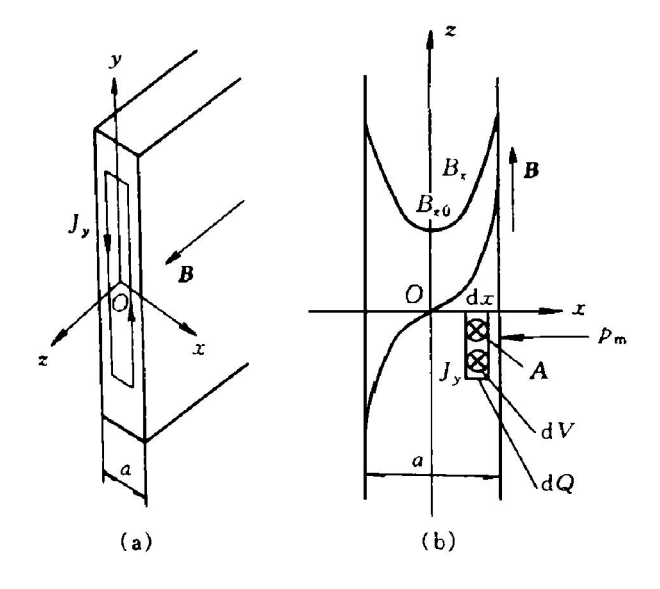


Fig. 1 Scheme of distributions of magnetic flux density B_z and current density J_y

conductivity of melt respectively.

As shown in Fig. 1(b), the power produced by induced current in dV with a bottom area A = 1 and a thickness dx is

$$dQ = \frac{J_{\gamma}^2}{\gamma} (1dx)$$
 (3)

Substituting equation (1) into equation (3), the result is

$$dQ = B^2 \frac{2 \Im f}{\mu(\operatorname{ch} K a + \cos K a)} \bullet (\operatorname{ch} 2K x - \cos 2K x) dx$$
 (4)

The heat energy produced in volume V with bottom area A=1 and thickness a is

$$Q = 2 \int_0^{a/2} \mathrm{d}Q \tag{5}$$

Substituting equation (4) into equation (5) the whole power produced in volume V is

$$Q = B^2 \frac{2 \mathbb{I} f}{\mathbb{I} K} \frac{\sinh Ka - \sin Ka}{\cosh Ka + \cos Ka}$$
 (6)

The average power produced in unit volume is

$$Q_0 = \frac{Q}{V} \tag{7}$$

Substitute $V = 1 \cdot a$ and equation (6) into equation (7), then

$$Q_0 = \frac{1}{a} \sqrt{\frac{4 \text{Jf}}{\mu^3}} \frac{\sinh Ka - \sin Ka}{\sinh Ka + \cos Ka} B^2$$
 (8)

For comparing the contributions of magnetic flux density to heating and to shaping, the $Q_0/p_{\rm m}$, ratio of average power absorbed by melt in unit volume to electromagnetic pressure on unit area, is defined as "ratio of heat to pressure". This ratio reflects the heating ability on melts in different confinements and shaping systems while the electromagnetic pressures on melt is the same. From equations (8) and (2), we can obtain

$$\frac{Q_0}{p_{\rm m}} = \frac{\sinh Ka - \sin Ka}{\int_0^{Ka} (\cosh^2 t - \cos^2 t)^{1/2} dt} \frac{4}{a} \sqrt{\frac{\pi f}{\mu_{\rm Y}}}$$
(9)

The results of numerical integration of equation (9) is shown in Fig. 2 and Fig. 3, which give the relationships between ratio of heat to pressure Q_0/p_m and thickness a, and electromagnetic parameter μ_{γ} of melt and current frequency f. These curves present that the ratio decreases with the decrease of current frequency and with the increases of thickness and electromagnetic parameter of melt. When the melt thickness is big or the frequency is low or the electromagnetic parameter is large, the ratio is small and the melt absorbs less heat while there exerts the same electromagnetic pressure on it, so an adjustment on magnetic field has a negligible effect on the temperature of melt. This conclusion is in good agreement with the results in the electromagnetic casting of big aluminum ingot. Inversely, if the melt thickness is thin or the frequency is high or the electromagnetic parameter is small, the ratio is big and the melt will absorb a lot of heat while there exerts the same electromagnetic pressure on it. The magnetic field can not only confine and shape the melt but also melt and heat the alloy simultaneously. It is obvious that in order to hold the electromagnetic confinement and

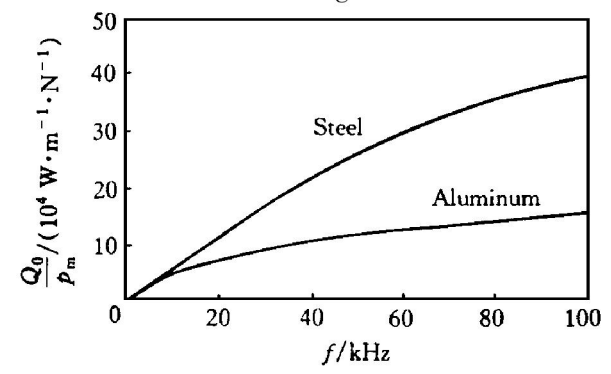


Fig. 2 $Q_0/p_m - f$ curves for plates of aluminum melt($\mu_Y = 5.03 \,\mathrm{H} \cdot \Omega^{-1} \cdot \mathrm{m}^{-2}$) and steel melt ($\mu_Y = 0.84 \,\mathrm{H} \cdot \Omega^{-1} \cdot \mathrm{m}^{-2}$) at thickness $a = 6 \,\mathrm{mm}$

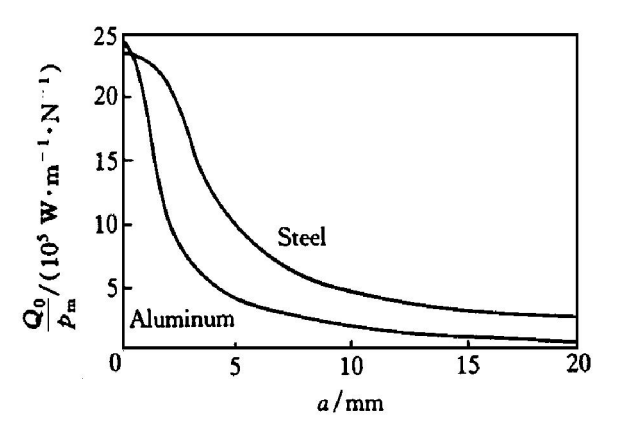


Fig. 3 $Q_0/p_m - a$ curves for plates of aluminum melt($\mu_Y = 5.03 \,\mathrm{H} \cdot \Omega^{-1} \cdot \mathrm{m}^{-2}$) and steel melt ($\mu_Y = 0.84 \,\mathrm{H} \cdot \Omega^{-1} \cdot \mathrm{m}^{-2}$) at frequency $f = 300 \,\mathrm{kHz}$

shaping process of thin plate like parts, a stable and wide coupling between melt shape and temperature field is necessary.

3 EXPERIMENTAL AND DISCUSSION

The factors which affect the coupling between shape and temperature field of thin plate melt have been investigated by the following experiments.

AF2. 5% Cu plate samples with a cross-section of 6 mm × 18 mm are selected in experiments. The frequency of electric current through the coil was 300 kHz. Experimental apparatus is illustrated in Fig. 4. Experiments were proceeded in two kinds of induction coils with a trumpet inside wall (H = 24 mm, α = 10°) and a vertical inside wall (H = 24 mm, $\alpha =$ 0), respectively. The position of solid/liquid interface was controlled by adjusting the coolant volume of flow. The melt shapes and positions of S/L interface and melt top were quenched and fixed by abruptly augmenting the coolant volume of flow and then measured. The distributions of magnetic flux density in space were measured with a detection coil made by us. The temperature profiles in melt along axis were measured with some thermal couples of 0.3 mm in diameter.

Curve No. 1 and curve No. 2 in Fig. 5 are the profiles of magnetic flux density measured along periphery of samples before melting in the coils with a trumpet inside wall and a vertical inside wall, respectively. The solid curves in Fig. 6 and Fig. 7 present the electromagnetic pressure profiles along sample per

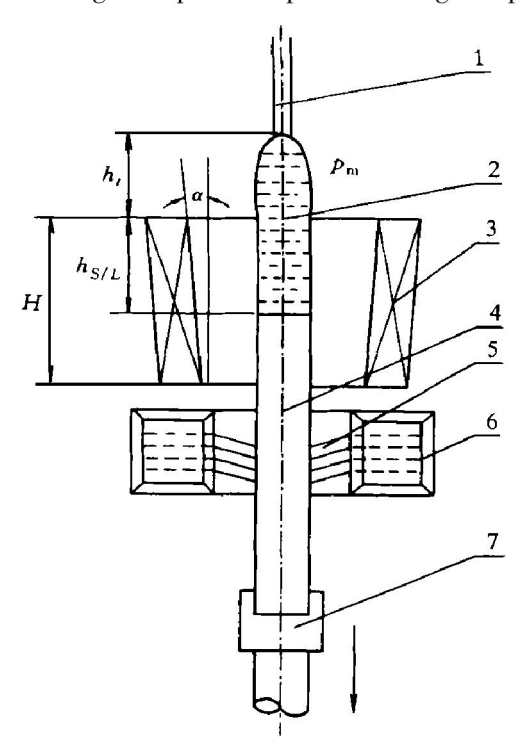


Fig. 4 Schematic diagram of experimental apparatus for electromagnetic confinement and shaping process 1—Solid material; 2—Melt; 3—Induction coil;

4 — Solidified part; 5 — Coolant; 6 — Cooler; 7 — Drawing bar

riphery, which are respectively calculated from curve No. 2 and curve No. 1 in Fig. 5 with equation (2). The dashed curves in Fig. 6 are the electromagnetic pressure profiles along sample periphery in coil with vertical inside wall while the electric current through the coil is decreased. The straight lines in two figures are the static pressure distributions of melts with different top positions. From the curves in Fig. 6, it can

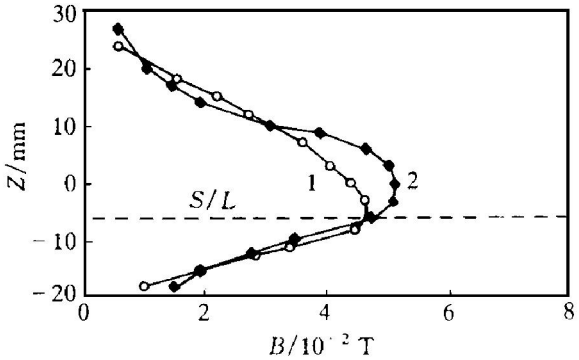


Fig. 5 Profiles of magnetic flux density measured along periphery of samples in different coils $1-\alpha=10^\circ$; $2-\alpha=0$

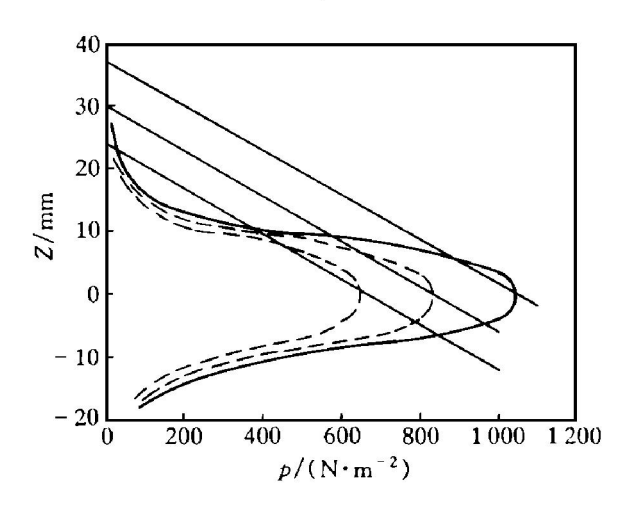


Fig. 6 Distributions of electromagnetic pressure $p_{\rm m}$ and static pressure $p_{\rm s}$ along sample periphery in coil with vertical inside wall

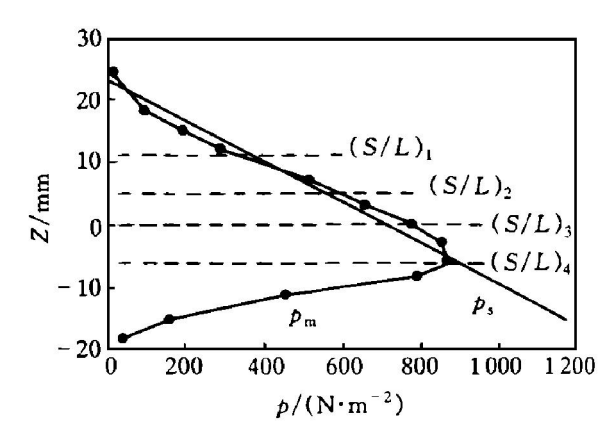


Fig. 7 Distributions of electromagnetic pressure $p_{\rm m}$ and static pressure $p_{\rm s}$ along sample periphery in coil with trumpet inside wall (α = 10°)

be seen that for coil with a vertical inside wall, wherever the position of S/L interface and the position of melt top are, and whatever the value of current density in the coil is, the electromagnetic pressure and static pressure always do not coincide well. The imbalance between static pressure and electromagnetic pressure will cause a deformation of melt, therefore the melt periphery is not vertical. Fig. 8(a) shows the melt shape of guenched sample obtained in this kind of induction coil. Usually, the melt with this periphery is not stable and the movement of S/L interface caused by a fluctuation of temperature results in a non-uniform cross-section or even process failure. But for induction coil with a 10° trumpet inside wall, if the positions of S/L interface and melt top are properly selected (in present experiment, $h_t = 11$ mm, $h_{S/L}$ = 18 mm) the electromagnetic pressure coincides with static pressure at every point on periphery quite well, so the melt has an ideal vertical periphery. On this condition, even if a quite big fluctuation of temperature has caused S/L interface to move in a wide range (as shown in Fig. 7, from position 1 to position 4, S/L interface moves about 17 mm), the good coincidence between electromagnetic pressure and static pressure always exists, thus the periphery of melt keeps vertical. Fig. 8(b) shows the photographs of melt shapes fixed by quenching while S/L interface reaches different positions. They explain that the melt shape and temperature field keep a good and stable coupling in a quite wide range, so the solidified samples have uniform cross-sections and smooth surfaces. Fig. 9 shows a series of samples obtained under this condition, which are well shaped and have smooth surfaces, elliptic cross-sections and unidirectional crystals.

The temperature profile in Fig. 10, where $T_{\rm m}$ is the temperature of liquidus, shows that the temperature gradient ($G_{\rm L}$) in the front of S/L interface increases with the decrease of position of S/L interface, and wherever the position of S/L interface is,

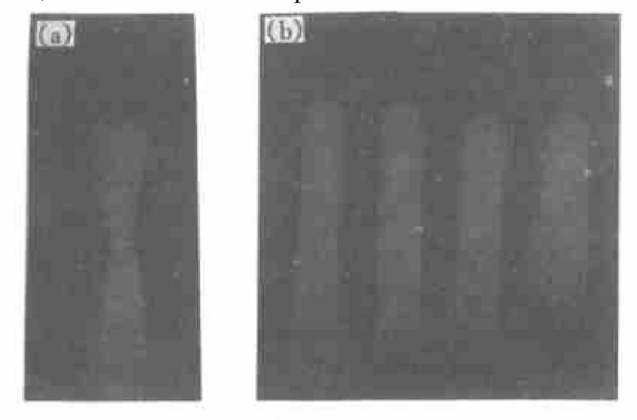


Fig. 8 Photographs of melt shapes (a) —Best melt shape quenched in coil with $\alpha = 0^{\circ}$; (b) —Melt shape quenched at different S/L interfaces in coil with $\alpha = 10^{\circ}$

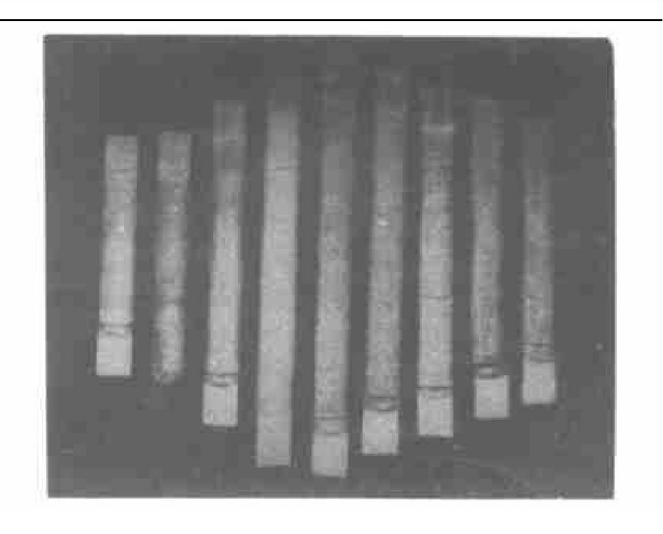


Fig. 9 Samples shaped in coil with trumpet inside wall ($\alpha = 10^{\circ}$)

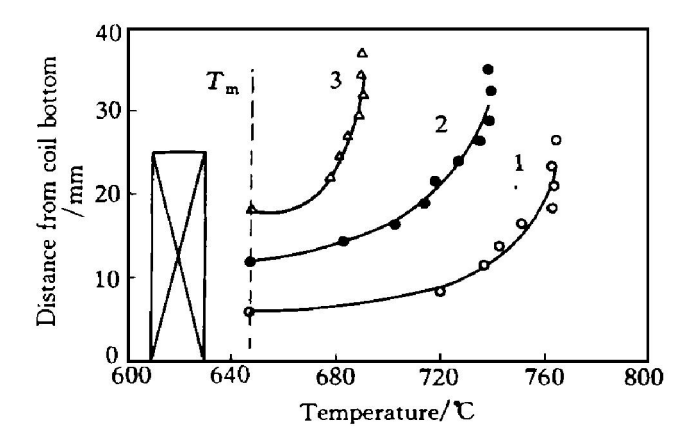


Fig. 10 Temperature profiles in melt for different positions of solid/liquid interface $1-G_{\rm L}=284$ °C/cm; $2-G_{\rm L}=140$ °C/cm; $3-G_{\rm L}=77$ °C/cm

the melt periphery is always vertical as shown in Fig. 8(b). That is, there is a stable and wide coupling between melt shape and temperature gradient. The wide variation range of temperature gradient makes the solidified structures of alloy have different forms and fineness. Especially as the high temperature gradient ahead of S/L interface is selected the solidified structures of alloy will have superfine unidirectional crystals which have excellent mechanical properties [11].

4 CONCLUSIONS

The theoretical analyses and experimental results show that if a low current frequency or a big electromagnetic parameter or a large thickness of melt is selected, the ratio of heat to pressure becomes small and the adjustment for melt shape or for temperature field has no obvious effect on another. Thus the control for the confinement and shaping process is relatively easy. But if the frequency is high or the melt thick-

ness is thin or the electromagnetic parameter is small, the ratio of heat to pressure is big. On this condition, the melting and shaping of melt can be completed sirmultaneously by a single induction coil. This is an advantage in the case of high ratio of heat to pressure. On the other hand, the big ratio asks the design on induction coil and the selection on the values of parameters which affect this process to produce a good and wide coincidence between static pressure and electromagnetic pressure. The wider the coincidence range is, the more stable and better the melt shape is. In this situation, the coupling range between temperature and melt shape can be wide and the temperature gradient in the front of S/L interface can be adjusted in a large range, which is the guarantee for confining and shaping a thin plate-like parts with a single induction coil successfully.

TABLE OF SYMBOLS

p _m ─Electromagnetic pressure;

 p_s —Static pressure by melt;

B —Value of magnetic flux density on melt surface:

 B_z —Value of magnetic flux density in melt;

 B_{z0} —Value of magnetic flux density at the center (x = 0) of melt;

 J_{γ} —Electric current density in melt;

i-Imaginary operator of complex number;

µ—Magnetic conductivity of melt;

Y —Electric conductivity of melt;

μγ —Electromagnetic parameter;

a —Melt thickness;

f —Electric current frequency;

 Q_0 —Average power produced in unit volume;

 Q_0/p_m —Ratio of heat to pressure;

 $G_{\rm L}$ —Temperature gradient in the front of S/L interface;

 $T_{\rm m}$ —Temperature of liquidus; $K = \sqrt{\pi f \mu_{\rm Y}}$

[REFERENCES]

- [1] Sautebin R and Haller W. Industrial application of electromagnetic casting of aluminum [J]. Light Metal Age, 1985, 14(8): 14.
- [2] Tyler D E, Lewis B G and Renschen P D. Electromagnetic casting of copper alloy [J]. Journal of Metals, 1985, 37(9): 51.
- [3] Mitsuaki Furui and Yo Kojima. Fabrication of small aluminum ingot by electromagnetic casting [J]. ISIJ International, 1993, 33(3): 400.
- [4] Kageyama R and Evans J W. A mathematical model for dynamic behavior of melts subjected to electromagnetic forces [J]. Metallurgical and Materials Transaction B, 1998, 29(8): 919.
- [5] Sears J W. Current processes for cold wall melting of tranium [J]. Journal of Metals, 1990, 42(3): 17.
- [6] Li B Q, Evans J W and Cook D P. An improved mathematical model for electromagnetic casters and testing by a physical model [J]. Metallurgical Transactions B, 1991, 22(2): 121.
- [7] El-Kaddah N and Mortimer J H. New crucibleless melting process promises refractory free melting for high-quality castings [J]. Light Metal Age, 1988, 17(10): 37.
- [8] Sakane J, Li B Q and Evans J W. Mathematical modeling of meniscus profile and melt flow in electromagnetic castings [J]. Metallurgical Transactions B, 1988, 19 (6): 397.
- [9] Shen J, Fu H Z, LI J G, et al. Analysis for electromagnetic pressure on thin plate melt [J]. The Chinese Journal of Nonferrous Metals, 1999, 9(7): 32.
- [10] Shen J, LI J S, LI J G, et al. Some characteristics of liquid melt meniscus in electromagnetic field [J]. Trans Nonferrous Met Soc China, 1995, 5(4): 64.
- [11] SHI Z X and FU H Z. Effect of solidification interface morphologies on microstructures of a Nirbase superalloy [J]. Chin J Met Tchnol, 1990, 6(5): 150.

(Edited by PENG Chao qun)